OTS PRICE

XEROX $ 2.60 ph.

RE-7

SELECTION OF OPTICAL SIGHTINGS FOR POSITION DETERMINATION IN INTERPLANETARY SPACE

by

Robert G. Stern

April 1964

Note: This report is to be presented at the National Aerospace Electronics Conference of the Institute of Electrical and Electronics Engineers on 12 May 1964 in Dayton, Ohio.

EXPERIMENTAL ASTRONOMY LABORATORY

MASSACHUSETTS INSTITUTE OF TECHNOLOGY

CAMBRIDGE 39, MASSACHUSETTS

Prepared for Publication by Jackson & Moreland

ABSTRACT

20586

A self-contained optical system for the determination of position in interplanetary space is examined. The measured quantities are the angles between pairs of celestial bodies. The specific problem studied is the selection of the angles to be observed such that the uncertainty in position estimation, due to noise in the measurements, is minimized.

The approach used is geometric. To reduce the amount of fuel required, practical interplanetary vehicles will move in trajectories that lie close to the ecliptic plane. The planets also move in orbits that lie close to the ecliptic plane. Because of these considerations, it is possible to choose the stars used in the optical sightings in such a manner that the determination of vehicle position in the nominal trajectory plane is only loosely coupled to the determination of position normal to the nominal plane. Moreover, such a choice of stars leads to a relatively accurate determination of position.

For the determination of vehicle position in the nominal trajectory plane, stars whose lines of sight lie close to the ecliptic plane are used; for position determination normal to the nominal plane a star whose line of sight is approximately normal to the ecliptic is required.

A survey is made of all first-magnitude stars to determine which are most useful for navigation purposes. Five of these stars have celestial latitudes between -10° and +10° and thus qualify for use in determination of in-plane position. The star Canopus is the most useful for out-of-plane position determination.

An example is presented which illustrates the selection procedure that has been formulated.

The procedure is so simple that the computations required can be carried out manually without undue strain; yet the resulting accuracy of vehicle position estimation is equivalent to that which can be expected from relatively elaborate computer programs that have previously been proposed.

A

AUTHOR

TABLE OF CONTENTS

SELECTION OF OPTICAL SIGHTINGS FOR POSITION DETERMINATION IN INTERPLANETARY SPACE

By: Robert G. Stern, Staff Engineer, M. I. T.

1. Introduction

The object of this paper is to develop a simple technique for selecting the optical sightings to be used in a self-contained navigation system for an interplanetary space vehicle. Three or more measurements of the angles subtended at the vehicle between the lines of sight to pairs of easily visible celestial bodies, if made in a relatively short time interval, can be used to compute the position of the vehicle at some specific time in the interval. Since all measurements are subject to some uncertainty, it is desired to pick those sightings which, for given uncertainties in the angular measurements, produce the smallest uncertainty in the computed estimate of position.

A general mathematical analysis of the use of an angular sighting in the determination of spatial position is presented in Appendix A; this problem has been treated in the literature by Larmore(1)* and by Haake and Welch(2), among others.

Battin(3) has used linear perturbation theory in the determination of position from angular sightings. A summary of this theory is contained in Appendix B.

The approach to be presented herein for selecting the sightings differs from previous approaches in that it exploits the peculiarly favorable geometric characteristics of practical interplanetary flight to produce a selection method that achieves the same order of accuracy as the previous methods in a somewhat simpler manner.

2. Background and Assumptions

A space vehicle is assumed to be in the midcourse phase of its journey between two planets. The nominal trajectory of the vehicle has been precomputed before the inception of the voyage. Due primarily to errors in the velocity of injection into the heliocentric orbit and secondarily to inaccuracy in the knowledge of the required astronautical constants, the vehicle's actual trajectory differs slightly from the reference trajectory. An on-board optical system, capable of measuring angles between lines of sight to celestial bodies, is used to determine position on the actual trajectory at a specified time.

The clock aboard the space ship is assumed to be ideal; therefore, the time of each measurement is known exactly. The position and velocity of the vehicle on the nominal trajectory, as well as the position and velocity of each of the planets, are known functions of time. The line of sight to each star used in the measurements is known; the effect of parallax on star sightings is neglected.

The specific angles to be measured and the time interval during which the measurements are to be made are preselected. The angles that would be measured if the vehicle were on the nominal trajectory and if the instrumentation were ideal are precomputed and stored in the on-board computer. The differences between actual and nominal angles are processed by the computer to produce an estimate of the vehicle's position deviation from the nominal trajectory at some instant of time in the measurement time interval.

3. Position Determination from Three Angular Measurements

In Appendix B linear perturbation theory is used to show that the variation of an on-board angular measurement from the nominal value that would be read if the vehicle were on its reference trajectory is related to the position variation of the vehicle at the time of the measurement by the vector equation

$$\delta A = \underline{h} \cdot \delta \underline{r} \qquad (3.1)$$

where δA is the angle variation, $\delta \underline{r}$ is the vector variation in vehicle position, and the geometry vector $\underline{h}$ is determined by the two bodies used in the angular sighting. (Underlining a symbol is used to signify a vector.)

*Superscript numerals enclosed in parentheses refer to similarly numbered items in the References.

When the nominal measurement angle A is the angle subtended at the vehicle by the lines of sight to two bodies in the solar system, $\underline{h}$ is given by

$$\underline{h} = \frac{\underline{n}_1}{z_1} + \frac{\underline{n}_2}{z_2} \tag{3.2}$$

where $\underline{n}_1$ and $\underline{n}_2$ are unit vectors in the plane containing angle A, the former perpendicular to the line of sight to body P_1 and the latter perpendicular to the line of sight to body P_2, as shown in Figure 1. $\underline{n}_1$ is positive in the direction in which P_1 would rotate in order to reduce the magnitude of A; similarly, $\underline{n}_2$ is positive in the direction in which P_2 would rotate to reduce the magnitude of A. Vectors $\underline{z}_1$ and $\underline{z}_2$, with magnitudes z_1 and z_2, are the position vectors of P_1 and P_2, respectively, relative to the nominal vehicle location at S.

The actual vehicle location at the nominal time of the measurement is S', which does not, in general, lie in the plane containing A. Thus, $\delta\underline{r}$ does not lie in this plane, and neither does the actual measurement angle $(A + \delta A)$.

From Equation (3.1), δA is equal to the component of $\delta\underline{r}$ in the direction of $\underline{h}$, divided by the magnitude of $\underline{h}$. It is shown in Appendix B that the magnitude of $\underline{h}$ is

$$h = \frac{2c}{z_1 z_2} \tag{3.3}$$

where 2c is the distance of P_2 from P_1.

When P_2 is a star, z_2 and 2c are effectively infinite. Equation (3.1) is still valid; Equations (3.2) and (3.3) reduce to

$$\underline{h}_i = \frac{\underline{n}_1}{z_1} \tag{3.2A}$$

$$h_i = \frac{1}{z_1} \tag{3.3A}$$

where the subscript i signifies that one of the sighted bodies is at infinite distance.

Three angle measurements, involving three different $\underline{h}$ vectors, are required to determine $\delta\underline{r}$. In matrix form, the relation of the three angle deviations to $\delta\underline{r}$ is

$$\begin{bmatrix} \delta A_1 \\ \delta A_2 \\ \delta A_3 \end{bmatrix} = \begin{bmatrix} \underline{h}_1^T \\ \underline{h}_2^T \\ \underline{h}_3^T \end{bmatrix} \delta\underline{r} \tag{3.4}$$

The vectors are all to be taken as column vectors. The superscript T denotes the transpose of a column vector or a matrix. In shorter notation, Equation (3.4) may be written as

$$\delta\underline{A} = \overset{*}{H}_3 \, \delta\underline{r} \tag{3.4A}$$

where the vector $\delta\underline{A}$ is the array of angle variations and $\overset{*}{H}_3$ is a three-by-three matrix. The asterisk over a capital letter signifies a matrix.

As long as $\overset{*}{H}_3$ is non-singular, (3.4A) can be solved for $\delta\underline{r}$.

$$\delta\underline{r} = \overset{*}{H}_3{}^{-1} \, \delta\underline{A} \tag{3.5}$$

where the superscript -1 denotes the inverse of a matrix.

The accuracy of the estimate of $\delta\underline{r}$ obtained from (3.5) depends primarily on the accuracy of the angle-measuring equipment. There is also a small position inaccuracy due to inaccuracy in the space vehicle's clock; the latter effect is neglected in this analysis. Let $\delta\tilde{A}$ be the value of the angle variation inferred from an angular measurement and δA be the "true" angle variation. The difference between the two is α, the uncertainty in the measurement.

$$\delta\tilde{A} = \delta A + \alpha \tag{3.6}$$

For the three measurements used in computing $\delta\underline{r}$, the following vector equation may be written:

$$\delta\underline{\tilde{A}} = \delta\underline{A} + \underline{\alpha} \tag{3.7}$$

The three elements of $\underline{\alpha}$ are random variables that are assumed to be normally distributed with zero means. The individual elements are assumed to be independent of each other. The standard deviation of each element is assumed to be known a priori. The covariance matrix of the measurement uncertainties is an indicator used to assess the accuracy of the estimate of position from the three angular sightings. This three-by-three symmetric matrix, designated $\overset{*}{U}_3$, is defined as follows:

$$\overset{*}{U}_3 = \langle \underline{a}\,\underline{a}^T \rangle = \begin{bmatrix} \langle a_1^2 \rangle & \langle a_1 a_2 \rangle & \langle a_1 a_3 \rangle \\ \langle a_2 a_1 \rangle & \langle a_2^2 \rangle & \langle a_2 a_3 \rangle \\ \langle a_3 a_1 \rangle & \langle a_3 a_2 \rangle & \langle a_3^2 \rangle \end{bmatrix} \tag{3.8}$$

Subscripts 1, 2, and 3 inside the matrix refer to the individual measurements. The angular brackets indicate the average value of the bracketed quantity. Since the uncertainties are uncorrelated and have zero means, $\overset{*}{U}_3$ is a diagonal matrix.

The estimated position variation vector is designated $\delta\underline{\tilde{r}}$ to distinguish it from the true position variation $\delta\underline{r}$. The difference between the two is the position uncertainty vector $\underline{\epsilon}$.

$$\delta\underline{\tilde{r}} = \delta\underline{r} + \underline{\epsilon} \tag{3.9}$$

By analogy with Equation (3.5), $\underline{\epsilon}$ is related to $\underline{a}$ by the equation

$$\underline{\epsilon} = \overset{*}{H}_3^{-1}\,\underline{a} \tag{3.10}$$

The covariance matrix of the uncertainty in position is

$$\begin{aligned} \overset{*}{E} &= \langle \underline{\epsilon}\,\underline{\epsilon}^T \rangle = \langle \overset{*}{H}_3^{-1}\,\underline{a}\,\underline{a}^T (\overset{*}{H}_3^{-1})^T \rangle \\ &= \overset{*}{H}_3^{-1}\,\overset{*}{U}_3\,(\overset{*}{H}_3^{-1})^T \end{aligned} \tag{3.11}$$

For most practical cases the assumed standard deviation is the same for all angular measurements. Then,

$$\langle a_1^2 \rangle = \langle a_2^2 \rangle = \langle a_3^2 \rangle = \sigma^2 \tag{3.12}$$

where σ is the standard deviation expressed in radians. When (3.12) is valid, Equations (3.8) and (3.11) reduce to

$$\overset{*}{U}_3 = \sigma^2\,\overset{*}{I}_3 \tag{3.8A}$$

$$\overset{*}{E} = \sigma^2\,(\overset{*}{H}_3^T\,\overset{*}{H}_3)^{-1} \tag{3.11A}$$

where $\overset{*}{I}_3$ is the three-by-three identity matrix.

Matrix $\overset{*}{E}$ is used in Sections 5 and 6 in the development of a specific criterion for the accuracy of the position estimate.

4. Position Determination from Redundant Measurements

When more than three measurements are used to determine vehicle position at time t, some statistical technique is used to obtain an optimal estimate. Potter and Stern[4] have shown that, under the assumption of Gaussian distribution of measurement uncertainties, two widely used techniques, one developed from maximum likelihood theory and the other from optimum filter theory, lead to the same estimate in position. When the measurement uncertainties are uncorrelated and have zero means, the maximum likelihood estimate is the same as that obtained from the method of least squares.

For N measurements, N being greater than three,

$$\begin{bmatrix} \delta A_1 \\ \vdots \\ \delta A_N \end{bmatrix} = \begin{bmatrix} \underline{h}_1^T \\ \vdots \\ \underline{h}_N^T \end{bmatrix} \delta\underline{r} \tag{4.1}$$

In the simpler notation

$$\delta\underline{A} = \overset{*}{H}_N\,\delta\underline{r} \tag{4.1A}$$

where $\delta\underline{A}$ is a vector with N components and $\overset{*}{H}_N$ is a matrix with N rows and three columns. The covariance matrix $\overset{*}{U}_N$ of the measurement uncertainties is the N-by-N symmetric matrix given by

$$\overset{*}{U}_N = \langle \underline{a}\,\underline{a}^T \rangle \tag{4.2}$$

From Reference (4) the maximum likelihood estimate of $\delta\underline{r}$ is

$$\delta\underline{\tilde{r}} = \overset{*}{F}\,\delta\underline{A} \tag{4.3}$$

where the filter matrix $\overset{*}{F}$ is defined as

$$\overset{*}{F} = (\overset{*}{H}_N^T\,\overset{*}{U}_N^{-1}\,\overset{*}{H}_N)^{-1}\,\overset{*}{H}_N^T\,\overset{*}{U}_N^{-1} \tag{4.4}$$

The error in the estimate is

$$\underline{\epsilon} = \overset{*}{F}\,\underline{a} \tag{4.5}$$

and the covariance matrix associated with $\underline{\epsilon}$ is

$$\overset{*}{E} = \langle \underline{\epsilon}\,\underline{\epsilon}^T \rangle = \overset{*}{F}\,\overset{*}{U}_N\,\overset{*}{F}^T = (\overset{*}{H}_N^T\,\overset{*}{U}_N^{-1}\,\overset{*}{H}_N)^{-1} \tag{4.6}$$

When the standard deviation of each measurement is equal to σ,

$$\overset{*}{U}_N = \sigma^2\,\overset{*}{I}_N \tag{4.2A}$$

$$\overset{*}{F} = (\overset{*}{H}_N^T\,\overset{*}{H}_N)^{-1}\,\overset{*}{H}_N^T \tag{4.4A}$$

$$\overset{*}{E} = \sigma^2\,(\overset{*}{H}_N^T\,\overset{*}{H}_N)^{-1} \tag{4.6A}$$

$\overset{*}{I}_N$ is the N-by-N identity matrix. Equations (4.2A) and (4.6A) are analogous to (3.8A) and (3.11A), respectively.

5. Statistical Theory

The probability density of the error vector $\underline{\epsilon}$ is defined as the joint probability density of the simultaneous occurrence of the three components of $\underline{\epsilon}$. With subscripts 1, 2, and 3 denoting the components of $\underline{\epsilon}$ and with p ( ) indicating the probability density of the argument within the parentheses,

$$p(\underline{\epsilon}) = p(\epsilon_1) \cdot p(\epsilon_2) \cdot p(\epsilon_3) \qquad (5.1)$$

The points on the locus of constant $p(\underline{\epsilon})$ form a closed surface centered at $\underline{\epsilon} = \underline{0}$. This surface is an ellipsoid, known as the equi-probability ellipsoid.

$p(\underline{\epsilon})$ is related to the covariance matrix $\overset{*}{E}$ by the equation

$$p(\underline{\epsilon}) = \frac{\exp\left(-\frac{1}{2}\underline{\epsilon}^T \overset{*}{E}{}^{-1} \underline{\epsilon}\right)}{\left|(2\pi)^3 \left|\overset{*}{E}\right|\right|^{1/2}} \qquad (5.2)$$

where $\left|\overset{*}{E}\right|$ is the determinant of $\overset{*}{E}$. The equation of the equi-probability ellipsoid is obtained by equating the argument of the exponential in (5.2) to a constant.

$$\underline{\epsilon}^T \overset{*}{E}{}^{-1} \underline{\epsilon} = B^2 \qquad (5.3)$$

The probability that the tip of the vector $\underline{\epsilon}$ lies either within or on the surface of a given equi-probability ellipsoid is a constant. A particularly useful ellipsoid is that for which this probability is 0.5; this ellipsoid is known as the 50% probability ellipsoid. For it the value of B is 1.5382.

The volume of the equi-probability ellipsoid is

$$V = \frac{4}{3}\pi B^3 \left|\overset{*}{E}\right|^{1/2} \qquad (5.4)$$

For the 50% probability ellipsoid,

$$V_{0.5} = \frac{4}{3}\pi (1.5382)^3 \left|\overset{*}{E}\right|^{1/2} \qquad (5.5)$$

For the deterministic case, when only three angular measurements are made,

$$\left|\overset{*}{E}\right| = \left|\overset{*}{H}_3{}^{-1}\right| \cdot \left|\overset{*}{U}_3\right| \cdot \left|(\overset{*}{H}_3{}^{-1})^T\right| = \frac{\sigma_1^2\,\sigma_2^2\,\sigma_3^2}{\left|\overset{*}{H}_3\right|^2} \qquad (5.6)$$

where σ_1, σ_2, and σ_3 are the standard deviations of the three measurements. If all three measurements have the same standard deviation σ,

$$\left|\overset{*}{E}\right| = \frac{\sigma^6}{\left|\overset{*}{H}_3\right|^2} \qquad (5.6A)$$

When there are redundant measurements, the $\overset{*}{H}$ matrix is not square; hence, the separation of the determinant of the matrix product into the product of the determinants of the individual matrices cannot be effected.

$$\left|\overset{*}{E}\right| = \frac{1}{\left|\overset{*}{H}_N{}^T \overset{*}{U}_N{}^{-1} \overset{*}{H}_N\right|} \qquad (5.7)$$

When all measurements have equal σ's,

$$\left|\overset{*}{E}\right| = \frac{\sigma^6}{\left|\overset{*}{H}_N{}^T \overset{*}{H}_N\right|} \qquad (5.7A)$$

Either of two numbers may be used as a single figure of merit relating to the accuracy of the position estimate. The first of these, the spherical probable error SPE, is defined as the radius of the sphere whose volume is equal to $V_{0.5}$.

$$SPE = 1.5382 \left|\overset{*}{E}\right|^{1/6} \qquad (5.8)$$

The second, the root-mean-square error RMSE, is defined by the relation

$$\begin{aligned} RMSE &= 1.5382 \left(\frac{1}{3}\,\mathrm{tr}\,\overset{*}{E}\right)^{1/2} \\ &= 0.888\,(\mathrm{tr}\,\overset{*}{E})^{1/2} \end{aligned} \qquad (5.9)$$

where tr signifies the trace of a matrix. The RMSE is equal to the root-mean-square of the principal axes of the 50% probability ellipsoid.

Both the SPE and the RMSE are invariant under any orthogonal coordinate transformation. If such a transformation is performed to convert $\overset{*}{E}$ into the diagonal matrix $\overset{*}{D}$ and if the diagonal elements are designated d_i^2, d_j^2, and d_k^2, the principal axes of the 50% probability ellipsoid are equal to 1.5382 d_i, 1.5382 d_j, and 1.5382 d_k, respectively. The two error criteria are

$$SPE = 1.5382\,(d_i d_j d_k)^{1/3} \qquad (5.8A)$$

$$RMSE = 0.888\,(d_i^2 + d_j^2 + d_k^2)^{1/2} \qquad (5.9A)$$

If $d_i = d_j = d_k$, the ellipsoid reduces to a sphere, and

$$SPE = 1.5382\, d_i = RMSE \tag{5.10}$$

6. Selection of Sightings - General Considerations

For greatest accuracy of position estimation the angular sightings are to be chosen such that the elements of the diagonalized covariance matrix $\overset{*}{D}$ are as small as possible and as nearly equal as possible.

If three sightings, all with the same value of σ, are used, $\left| \overset{*}{H}_3{}^T \overset{*}{H}_3 \right|$ is to be maximized; this is achieved by making the $\underline{h}$ vectors as large in magnitude as possible and as nearly mutually orthogonal as possible. If it were possible to make the three vectors exactly orthogonal, each measurement would yield a component of $\delta\underline{r}$ in a direction perpendicular to the components determined from the other two measurements. The largest magnitudes of the $\underline{h}$ vectors are normally obtained from sightings on the celestial bodies nearest to the vehicle.

The projection of $\delta\underline{r}$ in the plane normal to the line of sight from the vehicle to the nearest celestial body can be determined with relatively high accuracy if the first two sightings measure the angles between the line of sight to the nearest body and the lines of sight to each of two stars, the stars selected being those for which the $\underline{h}$ vectors of the two sightings are as nearly perpendicular to each other as possible. Both $\underline{h}$ vectors are perpendicular to the unit vector, to be designated $\underline{a}$, which lies along the line of sight from the vehicle to the nearest body. To obtain any information about the component of $\delta\underline{r}$ parallel to $\underline{a}$, it is necessary that the third sighting involve a second near body; it may be a measurement of the angle between the second near body and the nearest body, between the second near body and some third near body, or between the second near body and a star. The third sighting is chosen to maximize $\left| \overset{*}{H}_3{}^T \overset{*}{H}_3 \right|$; normally it will be the sighting for which $\underline{h} \cdot \underline{a}$ is a maximum. (In this discussion, the possibility of measuring the nearest body's angular diameter has not been considered, because the vehicle's distance from the nearest body is assumed to be large enough so that little meaningful information can be obtained from such a measurement.)

Due to the fact that the component of $\delta\underline{r}$ parallel to the line-of-sight vector $\underline{a}$ is determined from a sighting on a body that is farther away than the nearest body, the uncertainty in this vehicle position component is greater, sometimes much greater, than the uncertainty in the components lying in the plane perpendicular to $\underline{a}$. Any redundant measurements that may be made are designed to maximize $\left| \overset{*}{H}_N{}^T \overset{*}{H}_N \right|$; normally this means that they are the sightings for which the values of $\underline{h} \cdot \underline{a}$ are maximized.

The foregoing discussion indicates that the selection of near bodies to be used in the sightings is fairly straightforward. The number of bodies that are "near" enough to supply accurate position data is limited; usually there are only two or three. The nearest may be used for two basic sightings; another near one is required for the third basic sighting. Optimum redundant sightings usually involve near bodies other than the nearest. The situation with regard to the selection of stars to be used in the sightings is much more complex. The number of stars easily visible and recognizable from the space vehicle is quite large. It is obviously impractical to try to formulate a selection procedure which attempts to consider all the possible sightings involving the two or three near bodies and all the easily recognizable stars. In the next section a selection technique is proposed in which only a relatively small number of sightings need be studied.

7. Selection of Sightings - Practical Considerations

There are two geometric considerations, both concerned with orientation relative to the ecliptic plane, that are of great significance in establishing an effective procedure for selecting sightings. In the first place, the group of bodies from which the near bodies are chosen consists of the sun, the brighter planets, and possibly the earth's moon (when the vehicle is near the earth). The sun is always in the ecliptic plane; the other near bodies all move in orbits whose planes are inclined only slightly to the ecliptic plane.

Secondly, in order to take full advantage of the rotational motion of the earth about the sun, all practical interplanetary trajectories lie in planes inclined only slightly to the ecliptic plane.

The consequence of these two factors is that the lines of sight from the vehicle to each of the near bodies used in the sightings are, under most circumstances, at small inclinations to the ecliptic plane. This generalization is not valid during the launch phase, the terminal phase, or the flyby phase of an interplanetary mission, when the vehicle is very close to one planet, but it is valid in the midcourse phase, and the selection procedure being developed is intended to be used primarily for position determination during midcourse.

If the lines of sight from the vehicle's nominal position to the near bodies were exactly in the ecliptic plane at all times, there would be the possibility of computing the component of position variation $\delta \underline{r}$ that is normal to the ecliptic plane completely independently of the computation of the two components of $\delta \underline{r}$ in the ecliptic plane. This could be accomplished if at least one visible star could be found whose line of sight is normal to the ecliptic plane and if at least one visible star could be found whose line of sight lies in the ecliptic plane.

The angle between the line of sight to a near body and the line of sight to an ecliptic pole star would be 90° if the vehicle were on its reference path, regardless of the time of the measurement. The plane of the measurement would be perpendicular to the ecliptic plane. In the vehicle-centered ecliptic (X_E Y_E Z_E) coordinate system, the geometry vector $\underline{h}$ would lie along the Z_E - axis, and any variation δA of the measured angle from 90° would be directly proportional to the component of $\delta \underline{r}$ along the Z_E - axis and independent of the components of $\delta \underline{r}$ in the ecliptic plane.

For the measurement of the angle between the line of sight to a near body and the line of sight to a star whose line is in the ecliptic plane, $\underline{h}$ would be in the ecliptic and perpendicular to the line to the near body. A measured angle variation δA would be proportional to that component of $\delta \underline{r}$ lying in the ecliptic and perpendicular to the line to the near body; it would be independent of the component of $\delta \underline{r}$ in the Z_E direction.

If the first two measurements were those described above and if the nearest body were used in both, two orthogonal components of $\delta \underline{r}$ would be determined, and the remaining component would be parallel to $\underline{a}$, the unit vector along the line of sight to the nearest body. This component would be in the ecliptic plane. To determine the third component, the third sighting would measure the angle between the lines of sight to two near bodies or between the lines of sight to a near body other than the nearest body and a star whose line is in the ecliptic plane. The star would normally be the same as the one used in the second sighting, although it could be any star whose line lies in the ecliptic. The particular sighting chosen for the third measurement would be the one for which the magnitude of $\underline{h} \cdot \underline{a}$ is a maximum.

Because the uncertainty in the estimate of the component of $\delta \underline{r}$ along $\underline{a}$ would be greater than the uncertainty in the other two components after the first three measurements were completed, any redundant measurements used would be taken from the group considered for the third measurement. Each succeeding sighting would be that one not yet selected for which the magnitude of $\underline{h} \cdot \underline{a}$ is greatest.

The idealized conditions mentioned in the preceding paragraphs never occur in practical cases. The nominal lines of sight from vehicle to near bodies do not lie exactly in the ecliptic plane. The lines of sight to none of the more prominent stars lie either exactly normal to or exactly in the ecliptic plane. Thus, the actual procedure for sighting selection is more involved than that indicated for the ideal situation.

The object of the first sighting is to minimize the uncertainty in the component of $\delta \underline{r}$ along the Z_E - axis. To accomplish this in a practical case, a survey is made of the brightest stars, and only those stars for which the magnitude of the celestial latitude is closest to 90° are considered. The $\underline{h}$ vector for the sighting involving the nearest body and each of these quasi-pole stars is computed. The sighting selected for the first measurement is that for which the magnitude of the component of h in the direction of Z_E is a maximum.

The second sighting is intended to minimize the uncertainty in the component of $\delta \underline{r}$ normal to the $\underline{h}$ vector for the first sighting and in the plane normal to $\underline{a}$. The stars considered for this sighting are those for which the magnitude of the celestial latitude is closest to 0°. The $\underline{h}$ vector of the sighting involving the nearest body and each of these "in-plane" stars is computed, and the selected sighting is the one for which the magnitude of the scalar product of the $\underline{h}$ vectors of the first two sightings is a minimum.

The third sighting and any redundant sightings are chosen to reduce the uncertainty in the component of $\delta \underline{r}$ along $\underline{a}$. Sightings involving available pairs of near bodies are considered, also sightings involving near bodies other than the nearest and the "in-plane" stars considered for the second sighting. The sightings selected are the ones with maximum magnitudes of $\underline{h} \cdot \underline{a}$.

It is conceivable that the configuration of the near bodies at the time of the measurement is such that after one or two redundant measurements the uncertainty in the component of $\delta \underline{r}$ along $\underline{a}$ is less than the uncertainty in other components. It would then be desirable to modify the selection procedure used for any additional measurements to favor the component of $\delta \underline{r}$ which then has the largest uncertainty. In the interest of simplicity, such a procedure is not considered here. In any case, it is assumed that the number of redundant sightings is small - normally not greater than three.

8. Survey of First-Magnitude Stars

The performance requirements of the space vehicle's optical system are simplified if only the relatively bright celestial bodies are used for the angular measurements. Therefore, only celestial bodies whose apparent brightness as seen from the vehicle is at least as great as that of the dimmest first-magnitude star will be considered. In the case of the near bodies this constraint presents no difficulty, since, if a body is near enough to be useful for measurement purposes, it is near enough so that its apparent brightness is at least equivalent to that of a first-magnitude star.

There are 22 first-magnitude stars, that is, stars whose brightness as seen from the solar system is greater than that of a star with apparent visual magnitude of 1.5. These stars have been studied to determine which are suitable as ecliptic "pole" stars and which are suitable as ecliptic "in-plane" stars. The results of the study are contained in Table 1, in which the stars are numbered in order of decreasing apparent brightness, the brightest being number one. The brightness data are taken from Table 11.II of Reference (5).

The computed data for each star consist of the direction cosines m_{xE}, m_{yE}, m_{zE} of the line-of-sight vector from the solar system to the star, expressed in the ecliptic coordinate system, and also the celestial longitude and the celestial latitude of the star. The computations are based on values of right ascension and declination taken from the section entitled "Mean Places of Stars, 1962.0" in Reference (6). The value used for the obliquity of the ecliptic is 23.444 degrees. Figure 2 is a polar plot of the star locations on the celestial sphere.

Canopus, the second brightest star, is best situated to be an ecliptic pole star. Other possibilities, for each of which the magnitude of the celestial latitude is approximately 60 degrees, are Vega (5), Deneb (19), and Achernar (9). Five of the stars are at celestial latitudes between -10° and +10° and thus are considered useful as ecliptic in-plane stars. In order of increasing magnitude of latitude they are Regulus (21), Spica (16), Antares (15), Aldebaran (13), and Pollux (18).

9. Selection of Sightings - A Detailed Procedure

On the basis of the foregoing discussion it is now possible to formulate in detail a method for selecting the angular sightings to be used for position determination.

The sightings to be considered for the first measurement are

1. Nearest body - Canopus
2. Nearest body - Vega
3. Nearest body - Deneb
4. Nearest body - Achernar

Table 1. Characteristics of first magnitude stars.

Star Number	Star Name	Apparent Visual Magnitude	Direction Cosines in Ecliptic Coordinate System			Celestial Longitude (degrees)	Celestial Latitude (degrees)
			m_{x_E}	m_{y_E}	m_{z_E}		
1	Sirius	−1.43	−0.1806	0.7491	−0.6374	103.56	−39.60
2	Canopus	−0.73	−0.0610	0.2371	−0.9696	104.44	−75.83
3	α Centauri	−0.27	−0.3792	−0.6311	−0.6766	239.00	−42.58
4	Arcturus	−0.06	−0.7868	−0.3454	0.5115	203.70	30.76
5	Vega	0.04	0.1208	−0.4579	0.8808	284.78	61.73
6	Capella	0.09	0.1390	0.9109	0.3885	81.33	22.86
7	Rigel	0.15	0.2028	0.8317	−0.5169	76.30	−31.13
8	Procyon	0.37	−0.4102	0.8693	−0.2758	115.26	−16.01
9	Achernar	0.53	0.4915	−0.1338	−0.8605	344.77	−59.38
10	β Centauri	0.66	−0.4293	−0.5752	−0.6963	233.26	−44.13
11	Betelgeuse	0.4 to 1.0	0.0298	0.9606	−0.2762	88.22	−16.03
12	Altair	0.80	0.4522	−0.7456	0.4895	301.24	29.30
13	Aldebaran	0.75 to 0.95	0.3525	0.9309	−0.0953	69.26	− 5.47
14	α Crucis	0.87	−0.4531	−0.3987	−0.7973	221.34	−52.88
15	Antares	0.90 to 1.06	−0.3535	−0.9321	−0.0796	249.23	− 4.57
16	Spica	1.00	−0.9178	−0.3955	−0.0358	203.31	− 2.05
17	Fomalhaut	1.16	0.8335	−0.4187	−0.3605	333.32	−21.13
18	Pollux	1.16	−0.3831	0.9163	0.1163	112.69	6.68
19	Deneb	1.26	0.4537	−0.2134	0.8652	334.81	59.91
20	β Crucis	1.31	−0.4978	−0.4346	−0.7505	221.12	−48.63
21	Regulus	1.36	−0.8598	0.5105	0.0081	149.30	0.46
22	ϵ Canis Majoris	1.49	−0.2159	0.5858	−0.7811	110.23	−51.36

The sighting selected is that one for which $|\underline{h} \cdot \underline{k}|$ is a maximum, where $\underline{k}$ is a unit vector parallel to the ecliptic polar axis.

The sightings considered for the second measurement are

1. Nearest body – Regulus
2. Nearest body – Spica
3. Nearest body – Antares
4. Nearest body – Aldebaran
5. Nearest body – Pollux

The one selected is that for which $|\underline{h}_1 \cdot \underline{h}_2|$ is a minimum, where $\underline{h}_1$ is the geometry vector of the sighting already chosen from the first group and $\underline{h}_2$ is the geometry vector of the sighting to be chosen from the second group.

The third measurement is picked from the following set of sightings:

1. Nearest body – second nearest body
2. Nearest body – third nearest body
3. Second nearest body – third nearest body
4. Second nearest body – Regulus
5. Second nearest body – Spica
6. Second nearest body – Antares
7. Second nearest body – Aldebaran
8. Second nearest body – Pollux
9. Third nearest body – Regulus
10. Third nearest body – Spica
11. Third nearest body – Antares
12. Third nearest body – Aldebaran
13. Third nearest body – Pollux

The sighting selected is the one for which the projection of the geometry vector in the direction of the line of sight to the nearest body is of maximum length; i.e., the one for which $|\underline{h} \cdot \underline{a}|$ is a maximum.

If redundant measurements are used, they are to be chosen from among the sightings considered for the third measurement. The selection criterion is the same as that for the third measurement; the sightings selected are those for which $|\underline{h} \cdot \underline{a}|$ is largest.

It will be noted that a particular angle is never measured more than once, even though it may appear that repeated measurements of the same angle will result in a smaller volume of the equi-probability ellipsoid than that obtained from the suggested procedure. The reason is that the assumption of independent uncertainties, upon which this analysis is based, is hardly justifiable for repeated measurements. There is no practical method of filtering out unknown instrumentation biases or low-frequency random errors, which would usually have a more deleterious effect on accuracy if some of the measurements were repeated.

The proposed selection procedure involves the computation of a total of only twenty-two geometry vectors; each of the twenty-two is tested only once. It is for this reason that the procedure is regarded as simple; in fact, it is simple enough so that all the computations required for making the selections (not for determining the covariance matrix $\overset{*}{E}$ and the error criteria SPE and RMSE) can be performed manually on a desk calculator without undue strain.

10. Illustrative Example

To illustrate the selection procedure, a numerical example has been prepared. The basic data for the example are taken from Reference (3). Table 5.1 of the reference contains data for four interplanetary trajectories. The numerical example selects the sightings and computes the accuracy of the position estimate at a point on the fourth trajectory, an Earth-Venus trajectory for which the time of departure is April 19, 1964 and the time of flight is 0.30 year. The computations apply to vehicle position 0.20 year after launch.

Figure 3 shows the position components in the ecliptic plane of the lines of sight to the near bodies (Venus, Earth, and Sun) from the vehicle's nominal position. Also shown are the projections in the ecliptic plane of the lines of sight to the five in-plane stars. Table 2 shows the distances of the near bodies from the vehicle and the celestial latitudes of their lines of sight.

This numerical example is somewhat extreme from the standpoint of indicating the effectiveness of the new procedure. The trajectory is one that arrives at Venus when that planet is approximately at its maximum distance below the ecliptic plane; therefore the hyperbolic excess velocity at injection into the interplanetary orbit has an unusually large component in the direction normal to the ecliptic plane (-7529 feet per second). At the time of the measurements the vehicle is ten million kilometers below the ecliptic, and Venus, the nearest body, is three million kilometers below; the resulting inclination of 27.7° of the line of sight between the vehicle and Venus is a difficult test for a theory whose primary premise is that the lines of sight are inclined only slightly to the ecliptic.

Table 2. Data for Near Bodies.

Near Body	Distance from Vehicle (km)	Celestial Latitude of Line of Sight (deg)
Venus	14.8×10^6	27.7
Earth	37.6×10^6	15.5
Sun	121.9×10^6	4.7

The uncertainties in all angular measurements are assumed to be statistically independent with zero mean and standard deviation of 50 microradians (approximately 10.3 seconds of arc).

As a basis for comparison of the proposed selection procedure with some that have previously been employed, the accuracy of each of the six strategies shown on Page 252 of Reference (3) has also been computed. Six sightings are used in each of these strategies, and six have also been chosen in accordance with the new procedure. The sightings used are listed in Table 3.

The older strategies differ from the present proposal in several respects. Only the ten brightest stars are considered; since the brightest of the in-plane first-magnitude stars is number thirteen, Aldebaran, it is not possible for these strategies to utilize the in-plane and out-of-plane geometry upon which the present method is based. The overall strategy encompassing the six individual strategies requires the determination of the root-mean-square error for each of the six and the final selection of that one for which the RMSE is a minimum. No sighting is made on a star or planet whose line of sight lies within 15° of the line of sight to the sun; also, no measurement is made of the angle between the lines of sight to two planets. The selection procedures used in each of the six individual strategies are described on Pages 246 to 248 of Reference (3).

Table 3. Sightings Used for Position Determination

Strategy	First Body	Second Body
1	Venus	Rigel
	Venus	β Centauri
	Venus	Sun
	Earth	Capella
	Earth	Procyon
	Sun	Earth
2	Venus	Rigel
	Venus	β Centauri
	Venus	Sun
	Sun	Capella
	Sun	Rigel
	Sun	Earth
3	Sun	Capella
	Sun	Rigel
	Sun	Venus
	Venus	Rigel
	Venus	β Centauri
	Sun	Earth
4	Sun	Capella
	Sun	Rigel
	Venus	Sirius
	Venus	Capella
	Sun	Venus
	Sun	Earth
5	Sun	Capella
	Sun	Rigel
	Sun	Venus
	Venus	Achernar
	Venus	Procyon
	Sun	Earth
6	Earth	Capella
	Earth	Procyon
	Venus	Arcturus
	Sun	Earth
	Venus	β Centauri
	Sun	Venus
Proposed	Venus	Canopus
	Venus	Spica
	Earth	Sun
	Venus	Earth
	Earth	Pollux
	Earth	Regulus

The new method, as utilized in the present sample calculation, does not discriminate against sightings on bodies whose lines of sight are close to that of the sun (although it could easily be made to do so), and it permits measurements involving two planets. The star Pollux, used in the fifth sighting of the proposed strategy, would not have been used if the 15-degree criterion were in effect. Also, the fourth measurement is the angle between the lines of sight to two planets, Venus and Earth.

The amount of computation required by the older strategies is significantly greater than that for the new method, inasmuch as six different $\overset{*}{E}$ matrices must be determined and their traces compared before a final selection is made.

The numerical results of the investigation are shown in Table 4. For each strategy the data presented are the lengths of the three axes of the equi-probability ellipsoid, the spherical probable error, and the root-mean-square error. These data are given for the first three sightings of each set and also for all six sightings of each set.

When only three sightings are used, the proposed method results in a lower spherical probable error and a lower root-mean-square error than any of the previous methods. For six sightings the proposed method yields the lowest spherical probable error, but two of the six older methods give lower values of the root-mean-square error.

In the case of the six sightings, the choice of which strategy is "best" apparently depends on the criterion of "goodness." This anomalous situation is due to the fact that the axes of the equi-probability ellipsoid are so different in length; in each case the longest axis is at least five times as long as the shortest axis. None of the strategies are capable of equalizing the axis lengths. The RMSE criterion provides a heavy penalty if the axis lengths are considerably different; the SPE criterion does not. The axis lengths are so different in this example that a reasonable approximation to the RMSE can be obtained by neglecting the two smaller axes and simply multiplying the length of the long axis by 0.6.

It is the author's opinion that the RMSE is a better criterion for position accuracy than the SPE precisely because it is affected so strongly by the longest axis of the equi-probability ellipsoid. A cigar-shaped ellipsoid, with one long axis and two short axes, is generally less desirable from an accuracy viewpoint than a nearly spherical ellipsoid whose volume is slightly greater than that of the cigar-shaped one.

The configuration shown in Figure 3 indicates the interesting possibility that the sightings for the new procedure might be selected graphically, without any exact computation of geometry

Table 4. Numerical results for seven sighting strategies -- all distances in kilometers.

Strategy	Axes of Equi-Probability Ellipsoid			SPE	RMSE
	Largest axis	Middle axis	Smallest axis		
Three Sightings					
1	28,737	3,466	788	4,282	16,718
2	28,737	3,466	788	4,282	16,718
3	37,268	13,526	1,286	8,655	22,902
4	47,163	13,618	1,041	8,746	28,348
5	37,268	13,526	1,286	8,655	22,902
6	7,364	2,149	1,917	3,119	4,565
Proposed	6,092	1,840	958	2,207	3,716
Six Sightings					
1	5,074	1,379	752	1,739	3,067
2	5,575	1,779	778	1,976	3,408
3	5,575	1,779	778	1,976	3,408
4	5,731	1,763	800	2,007	3,493
5	13,191	1,882	671	2,553	7,703
6	4,424	1,382	850	1,732	2,721
Proposed	5,415	985	859	1,661	3,216

vectors. The first measurement, for which the sketch is not needed, would always be nearest body-Canopus (in this case Venus-Canopus). The second would pair the nearest body and the in-plane star whose line of sight is most nearly perpendicular to the line of sight to the nearest body; from the figure the bodies would be Venus and Spica. The remaining measurements would be those for which the geometry vectors, which could be sketched in graphically, would have the largest projections along the line of sight to the nearest body. They would involve combinations of near bodies, or the second nearest body and in-plane stars with lines of sight nearly perpendicular to the line to the second nearest body, or the third nearest body and in-plane stars whose lines of sight are nearly perpendicular to the line to the third nearest body. In this example the line of sight to the third nearest body, the sun, is nearly parallel to the line to the nearest body, Venus; therefore, sun-star measurements are not desirable. On the basis of these considerations, the additional measurements would be Earth-Regulus, Earth-Venus, Earth-Pollux, and Earth-Sun. Although not in the same order, this set of measurements is identical with that shown for the proposed strategy in Table 3.

11. Conclusion

By exploiting the fact that the lines of sight from the space vehicle to the nearest visible celestial bodies are normally inclined only slightly to the ecliptic plane, it has been possible to devise a simple, effective procedure for selecting the angular sightings to be used for determination of vehicle position. The amount of computation required to make the selections is relatively small. In fact, it is even possible to make a reasonably good choice of sightings graphically, with an absolute minimum of computation.

Despite the fact that the numerical example chosen provides an extreme test of the new selection procedure, the position accuracy obtained compares well with that obtained from previous methods. It is anticipated that even more favorable results may be obtained when the new procedure is used in less extreme cases, i. e., when the lines of sight from vehicle to near bodies have smaller inclinations to the ecliptic plane.

APPENDICES

A. Position Determination from On-Board Angular Sightings

Figure 4 illustrates the position, at some specified time, of a space vehicle relative to two "near" celestial bodies (i. e., members of the solar system). The vehicle is at point S; the two near bodies are at P_1 and P_2. The distances from the vehicle to the near bodies are $SP_1 = z_1$ and $SP_2 = z_2$. The distance between the near bodies is $P_1 P_2 = 2c$. The X - Y coordinate system in the figure lies in the plane of triangle $P_1 S P_2$, its origin is at P_1, and the X - axis lies along $P_1 P_2$. The position coordinates of the vehicle are (x, y). The auxiliary line SQ is perpendicular to $P_1 P_2$.

The angle to be measured from the vehicle is $\measuredangle P_1 S P_2$, which is designated A. This angle is related to x, y, and c as follows:

$$\tan A = \tan(\measuredangle P_1 SQ + \measuredangle QSP_2) = \frac{2cy}{(x-c)^2 + y^2 - c^2} \qquad (A.1)$$

The equation of the locus of points of constant A in the X - Y plane is

$$(x-c)^2 + (y - c\cot A)^2 = (c \csc A)^2 \qquad (A.2)$$

This is the equation of a circle with center at (c, c cot A) and radius equal to c csc A. Thus, the constant-measurement-angle loci in the X - Y plane are arcs of circles whose centers all lie on the perpendicular bisector of $P_1 P_2$. The three-dimensional constant-measurement angle loci are the surfaces generated by rotating the circular arcs about $P_1 P_2$; these surfaces are known as "navoids."

The gradient surfaces are surfaces perpendicular to the navoids. The equation of these surfaces can be obtained from the slope of the navoids. From Eq. (A-2) the slope of a constant-angle locus is

$$\left(\frac{dy}{dx}\right)_A = -\frac{x-c}{y - c\cot A} \qquad (A.3)$$

Then the slope in the X - Y plane of the gradient curve passing through (x, y) is

$$\tan \phi = \left(\frac{dy}{dx}\right)_G = -\left(\frac{dy}{dx}\right)_A^{-1} = \frac{(x-c)^2 - y^2 - c^2}{-2(x-c)\,y} \tag{A. 4}$$

where ϕ is the angle between the tangent to the gradient curve and the X - axis. In order to integrate this equation, the terms are rearranged as follows:

$$\frac{2(x-c)\,y\,dy - y^2\,dx}{(x-c)^2} = \left[\frac{c^2}{(x-c)^2} - 1\right] dx \tag{A. 5}$$

The integral is

$$\frac{y^2}{x-c} = -\frac{c^2}{x-c} - (x-c) + 2k \tag{A. 6}$$

where k is a constant of integration. After regrouping,

$$[x - (c+k)]^2 + y^2 = k^2 - c^2 = R^2 \tag{A. 7}$$

This is the equation of a circle with center at (c + k, 0) and radius $R = \sqrt{k^2 - c^2}$. The magnitude of the constant k must be larger than c, but it can have either a positive or a negative sign. Thus the gradient curves are circular arcs whose centers lie on that portion of the X - axis which is outside the line segment $P_1 P_2$. The three-dimensional gradient surfaces are the spheres obtained by rotating the semicircular arcs in the upper half of the X - Y plane about $P_1 P_2$.

Several constant-measurement-angle loci and gradient curves in the X - Y plane are illustrated in Figure 5.

From Figure 6 it may be seen that ϕ is equal to the angle between the Y - axis and the radius OS of the gradient circle. The center O of the gradient circle passing through S is the point at which the tangent to the constant-angle locus at S intersects the X - axis.

The sensitivity factor K associated with an angular sighting is defined as the magnitude of the ratio of the position error caused by a small error α in the angular measurement, to the value of α itself. $\tilde{A}$, the measured value of the angle, is related to A, the true value, by the equation

$$\tilde{A} = A + \alpha \tag{A. 8}$$

The position error due to α is in the direction of the tangent to the gradient circle at the point of the measurement and is equal in magnitude to the radius R of the gradient circle multiplied by β, the change in ϕ caused by α. Then,

$$K = \left|\frac{R\beta}{\alpha}\right| \tag{A. 9}$$

where the vertical bars signify the absolute value.

By taking first variations of the expressions already developed for A and ϕ, and utilizing the geometric relationships of Figure 6, it can be show that

$$\frac{\beta}{\alpha} = \frac{x-c}{c} \tag{A. 10}$$

Also,

$$R = \frac{cy}{|(x-c)| \sin A} \tag{A. 11}$$

so that

$$K = \frac{y}{\sin A} = \frac{z_1 z_2}{2c} \tag{A. 12}$$

No vertical bars are needed in Eq. (A. 12) because y, z_1, z_2, c, and sin A are all positive quantities.

The sensitivity factor is directly proportional to the distance of the vehicle from each of the two near bodies being sighted and inversely proportional to the distance of the near bodies from each other. To minimize the sensitivity factor, it is obviously desirable to use the nearest body in as many of the measurements as possible, subject to the constraints imposed by the three-dimensional nature of the position determination problem.

The angle between the line of sight to a near body and the line of sight to a star is simpler to analyze than the angle between the line of sight to two near bodies. In fact, the equations of the former can be obtained from those of the latter by letting z_2 and $2c$ approach infinity. To distinguish the characteristics of the near body-star measurement from those of the measurement involving two near bodies, the subscript i (signifying that one of the bodies is at infinite distance) will be appended to symbols referring to the near body-star measurement.

In Figure 7 the line of sight $P_1 B$ from near body to star is parallel to S T, the line of sight from vehicle to star. The measurement angle A_i is $\measuredangle TSP_1$ in the figure. The X and Y axes are shown, with the origin at P_1. The constant-measurement-angle locus in the X-Y plane is a straight line, passing through P_1, whose inclination to the positive X-axis is the supplement of A_i. The equation of the locus is

$$\frac{y}{x} = \tan(\pi - A_i) = -\tan A_i \qquad \text{(A. 13)}$$

The gradient curves in the X-Y plane are concentric circles centered at P_1. The equation of the gradient circle passing through S is

$$x^2 + y^2 = z_1^2 = R_i^2 \qquad \text{(A. 14)}$$

where the radius R_i is equal to z_1, the distance of the near body from the vehicle.

In three dimensions the constant-angle loci are cones with apex at P_1 and axis along P_1 B. If A_i lies between 0 and $\pi/2$ radians, the cone opens outward in the direction of the star, and its half-angle is equal to A_i. If A_i is between $\pi/2$ and π radians, the cone opens outward in the direction away from the star, and its half-angle is the supplement of A_i. The three-dimensional gradient surfaces are concentric spheres centered at P_1.

The inclination of the gradient circle at (x,y) to the positive X-axis is

$$\phi_i = \frac{\pi}{2} - A_i \qquad \text{(A. 15)}$$

Thus, the sensitivity factor K_i is

$$K_i = \left| \frac{R_i \beta_i}{\alpha_i} \right| = z_1 \qquad \text{(A. 16)}$$

Three independent angular measurements are required to determine spatial position of the vehicle as the common intersection of the three three-dimensional constant-angle loci. Since three measurements cannot be made simultaneously, provision must be made for determining the change in the lengths z_1, z_2, and c, and the change in the orientation of the plane of each measurement, as a function of time.

B. Linear Perturbation Theory

When the departure of a space vehicle from its reference trajectory is small throughout its flight, linear perturbation theory is well suited to the problem of position determination. Figure 8 illustrates the use of the theory in processing an angular sighting between two near bodies. If the space vehicle were on its reference trajectory, the measurement angle at time t would be $A = \measuredangle P_1 S P_2$. Because of instrumentation difficulties inherent in the simultaneous tracking of two moving celestial bodies, it is not practical to stipulate that the measurement be made exactly at time t. The measurement is actually made at time $(t + \tau)$, where τ is a relatively small time interval. The actual measurement angle is $(A + \delta A') = \measuredangle P_1' S' P_2'$.

The displacements of the three bodies at time $(t + \tau)$ from their nominal positions at time t are

$$\overline{SS'} = \delta \underline{r} + \underline{v}_S \tau \qquad \text{(B. 1)}$$

$$\overline{P_1 P_1'} = \underline{v}_{P_1} \tau \qquad \text{(B. 2)}$$

$$\overline{P_2 P_2'} = \underline{v}_{P_2} \tau \qquad \text{(B. 3)}$$

where $\delta \underline{r}$ is the position deviation of the vehicle from the reference trajectory at time t and the $\underline{v}$ vectors are velocities of the bodies with respect to the sun at time t.

The difference between the actual vector $\overline{S' P_1'}$ and the reference vector $\overline{S P_1}$ is

$$\delta \underline{z}_1' = S' P_1' - S P_1 = \delta \underline{z}_1 - (\underline{v}_S - \underline{v}_{P_1}) \tau \qquad (B.4)$$

where

$$\delta \underline{z}_1 = - \delta \underline{r} \qquad (B.5)$$

The magnitude of $\delta \underline{z}_1$ is

$$\delta z_1' = \frac{\underline{z}_1 \cdot \delta \underline{z}_1'}{z_1} \qquad (B.6)$$

Similar expressions can be written for $\delta \underline{z}_2'$, $\delta \underline{z}_2$, and $\delta z_2'$.

The scalar product of the vectors forming A is

$$S P_1 \cdot S P_2 = \underline{z}_1 \cdot \underline{z}_2 = z_1 z_2 \cos A \qquad (B.7)$$

The first variation of this equation, corresponding to the actual measurement angle $(A + \delta A')$, is

$$\begin{aligned}
&\underline{z}_1 \cdot \delta \underline{z}_2' + \underline{z}_2 \cdot \delta \underline{z}_1' \\
&= \underline{z}_1 \cdot \delta \underline{z}_2 + \underline{z}_2 \cdot \delta \underline{z}_1 - \tau \, [\underline{z}_1 \cdot (\underline{v}_S - \underline{v}_{P_2}) \\
&\qquad + \underline{z}_2 \cdot (\underline{v}_S - \underline{v}_{P_1})] \\
&= - z_1 z_2 \sin A \, \delta A' + z_2 \cos A \, \delta z_1' \\
&\qquad + z_1 \cos A \, \delta z_2' \\
&= - z_1 z_2 \sin A \, \delta A' + z_2 \cos A \, \frac{\underline{z}_1 \cdot \delta \underline{z}_1'}{z_1} \\
&\qquad + z_1 \cos A \, \frac{\underline{z}_2 \cdot \delta \underline{z}_2'}{z_2}
\end{aligned} \qquad (B.8)$$

The solution for $\delta A'$ is

$$\begin{aligned}
\delta A' = - \frac{1}{\sin A} \Bigg[& \frac{1}{z_1} (\underline{m}_2 - \underline{m}_1 \cos A) \cdot (\delta_{\underline{z}_1} - \underline{v}_{R_1} \tau) \\
& + \frac{1}{z_2} (\underline{m}_1 - \underline{m}_2 \cos A) \cdot (\delta_{\underline{z}_2} - \underline{v}_{R_2} \tau) \Bigg]
\end{aligned} \qquad (B.9)$$

where $\underline{m}_1$ and $\underline{m}_2$ are unit vectors along the lines of sight from S to P_1 and from S to P_2, respectively.

$$\underline{m}_1 = \frac{\underline{z}_1}{z_1} \qquad (B.10)$$

$$\underline{m}_2 = \frac{\underline{z}_2}{z_2} \qquad (B.11)$$

$\underline{v}_{R_1}$ and $\underline{v}_{R_2}$ are the relative velocity vectors of S with respect to P_1 and P_2.

$$\underline{v}_{R_1} = \underline{v}_S - \underline{v}_{P_1} \qquad (B\text{-}12)$$

$$\underline{v}_{R_2} = \underline{v}_S - \underline{v}_{P_2} \qquad (B\text{-}13)$$

Two new unit vectors $\underline{n}_1$ and $\underline{n}_2$ are defined by

$$\underline{n}_1 = \frac{1}{\sin A} (\underline{m}_2 - \underline{m}_1 \cos A) \qquad (B.14)$$

$$\underline{n}_2 = \frac{1}{\sin A} (\underline{m}_1 - \underline{m}_2 \cos A) \qquad (B.15)$$

$\underline{n}_1$ is in the plane of the nominal measurement (i.e., the plane containing P_1, S, and P_2) and is perpendicular to $\underline{m}_1$. The positive direction of $\underline{n}_1$ is the direction in which $\underline{m}_1$ would be rotated (through the angle A, which is less than π radians) to bring it into coincidence with $\underline{m}_2$. Similarly, $\underline{n}_2$ is perpendicular to $\underline{m}_2$ and positive in the direction in which $\underline{m}_2$ would be rotated to approach $\underline{m}_1$. With this new notation and with $-\delta \underline{r}$ substituted for both $\delta \underline{z}_1$ and $\delta \underline{z}_2$, Equation (B.9) becomes

$$\begin{aligned}
\delta A &= \delta A' - \tau \left(\frac{\underline{n}_1}{z_1} \cdot \underline{v}_{R_1} + \frac{\underline{n}_2}{z_2} \cdot \underline{v}_{R_2} \right) \\
&= \left(\frac{\underline{n}_1}{z_1} + \frac{\underline{n}_2}{z_2} \right) \cdot \delta \underline{r} \\
&= \underline{h} \cdot \delta \underline{r}
\end{aligned} \qquad (B.16)$$

δA is the "effective" angle variation, i.e., the angle variation due solely to $\delta \underline{r}$. The term containing τ in (B.16) can be computed directly, since τ for the given measurement is obtained from the clock reading and the coefficient of τ is a function of the reference trajectory, all of whose characteristics are know. Thus, the value $\delta A'$ obtained directly from the angular measurement can be adjusted to yield δA, the desired value.

The vector $\underline{h}$ in (B.16) is known as the "geometry vector."

$$\underline{h} = \frac{\underline{n}_1}{z_1} + \frac{\underline{n}_2}{z_2} \tag{B. 17}$$

The variation δA is a measure of the component of $\delta \underline{r}$ in the direction of $\underline{h}$. Obviously, three such components, in different directions, are needed to specify $\delta \underline{r}$ completely in three-dimensional space.

The magnitude of $\underline{h}$ is

$$h = (\underline{h} \cdot \underline{h})^{1/2} = \frac{2c}{z_1 z_2} \tag{B. 18}$$

since $\underline{n}_1$ and $\underline{n}_2$ are unit vectors and

$$\underline{n}_1 \cdot \underline{n}_2 = - \cos A \tag{B. 19}$$

As in Appendix A, 2 c is the distance of P_2 from P_1. By comparing (B. 18) with (A. 12), it can be seen that the magnitude of $\underline{h}$ is the reciprocal of the sensitivity factor K. Thus, a connection has been established between the perturbation approach and the geometric approach to the navigation problem. It can also be shown that the direction of $\underline{h}$ is parallel to the tangent to the gradient circle passing through the point S on the reference trajectory.

For the case of the measurement of the angle between a near body and a star, z_2 is infinite, and the geometry vector is then

$$\underline{h}_i = \frac{\underline{n}_1}{z_1} \tag{B. 20}$$

REFERENCES

1. Larmore, L., "Celestial Observations for Space Navigation," Aero/Space Engineering, Vol. 18, No. 1, Jan. 1959, pp. 37-42.

2. Haake, H. B. and Welch, J. D., "A Self-Contained Interplanetary Navigator," IRE Transactions on Aerospace and Navigational Electronics, Vol. ANE-8, No. 1, March 1961, pp. 28-41.

3. Battin, R. H., Astronautical Guidance, McGraw-Hill Book Company, Inc., N. Y., 1964.

4. Potter, J. E. and Stern, R. G., "Statistical Filtering of Space Navigation Measurements," Progress in Astronautics and Aeronautics, Vol. 13, R. C. Langford and C. J. Mundo editors, Academic Press, Inc., N. Y., in press.

5. Baker, R. H., Astronomy, Seventh Edition, D. Van Nostrand Co., Inc., Princeton, N. J., 1959.

6. The American Ephemeris and Nautical Almanac for the Year 1962, U. S. Government Printing Office, Washington, 1960.

ACKNOWLEDGEMENT

The preparation and presentation of this paper have been supported by the National Aeronautics and Space Agency under NASA Grant Ns G 254-62.

The author wishes to express his appreciation to Mr. Louis Kleiman, who wrote the computer program from which the numerical data in the illustrative example were obtained.

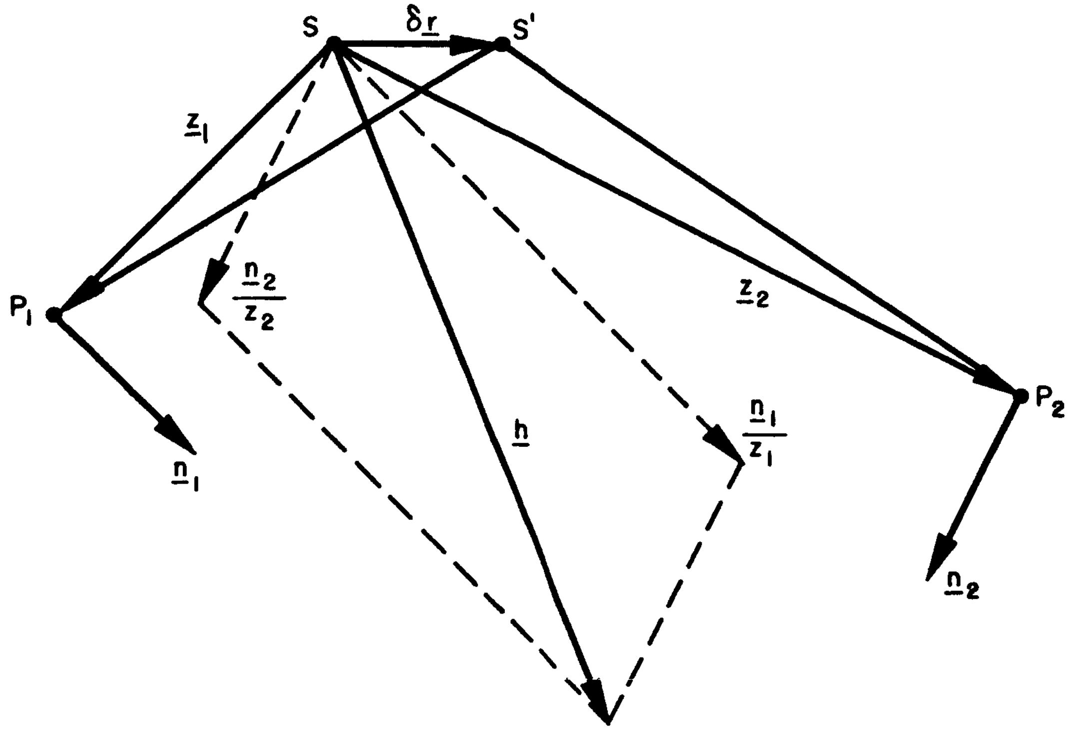

S	-	nominal space vehicle position
S'	-	actual space vehicle position
P_1, P_2	-	near body positions
$A = \measuredangle P_1 S P_2$	=	nominal measurement angle
$(A + \delta A) = \measuredangle P_1 S' P_2$	=	actual measurement angle
$\delta \underline{r} = \overline{SS'}$	=	position variation of space vehicle
$\underline{z}_1$, $\underline{z}_2$	-	position vectors of P_1 and P_2 relative to S
$\underline{n}_1$, $\underline{n}_2$	-	unit vectors normal to $\underline{z}_1$ and $\underline{z}_2$, respectively
$\underline{h}$	-	geometry vector for measurement angle A

Fig. 1. Geometry vector for measurement of angle between lines of sight to two near bodies.

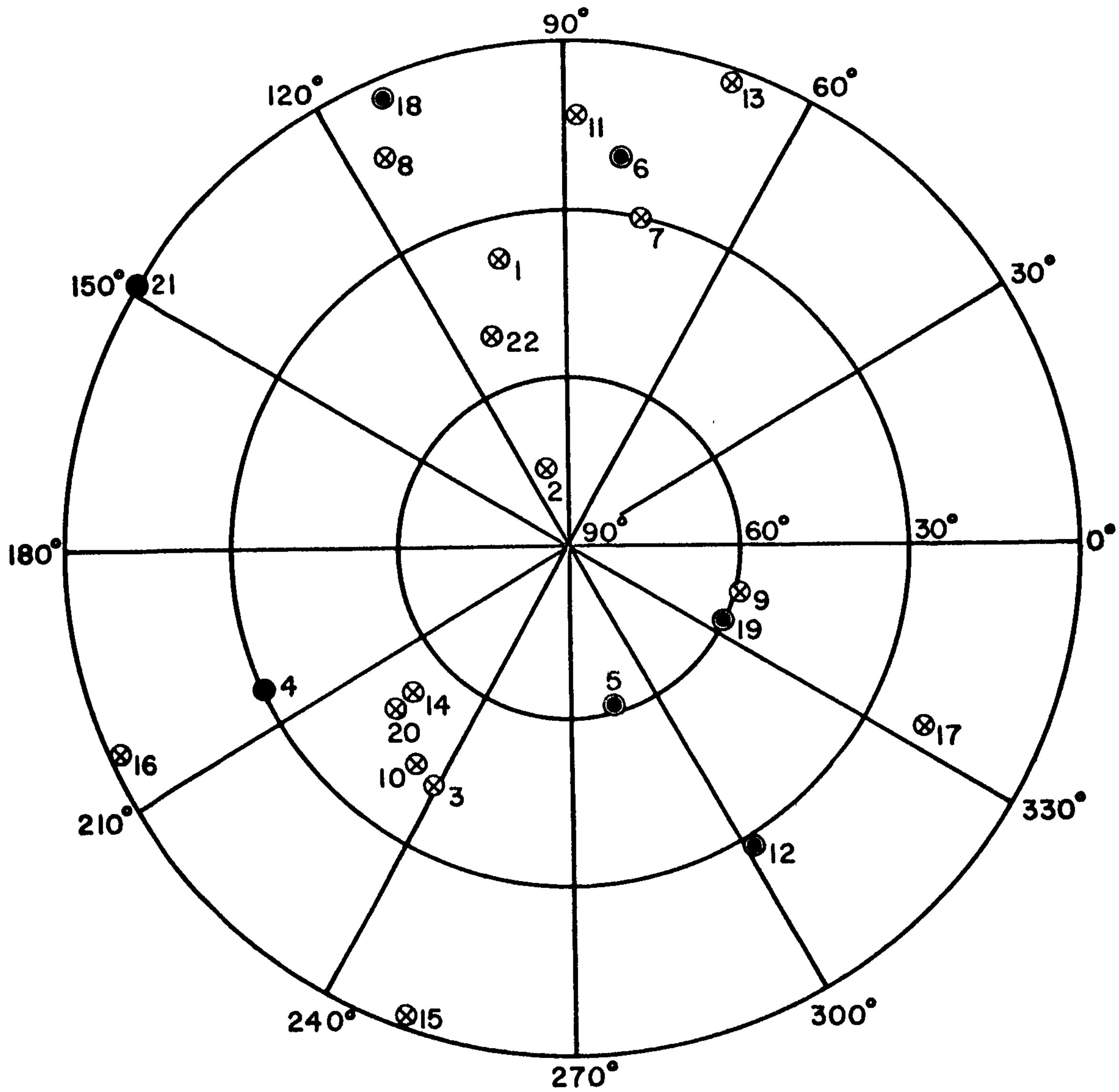

Numbers refer to stars listed in Table 1.

◉ Star at positive celestial latitude.

⊗ Star at negative celestial latitude.

Radial lines are loci of points of constant celestial longitude.

Concentric circles are loci of points of constant magnitude of celestial latitude.

Fig. 2. Celestial longitude and latitude of first magnitude stars.

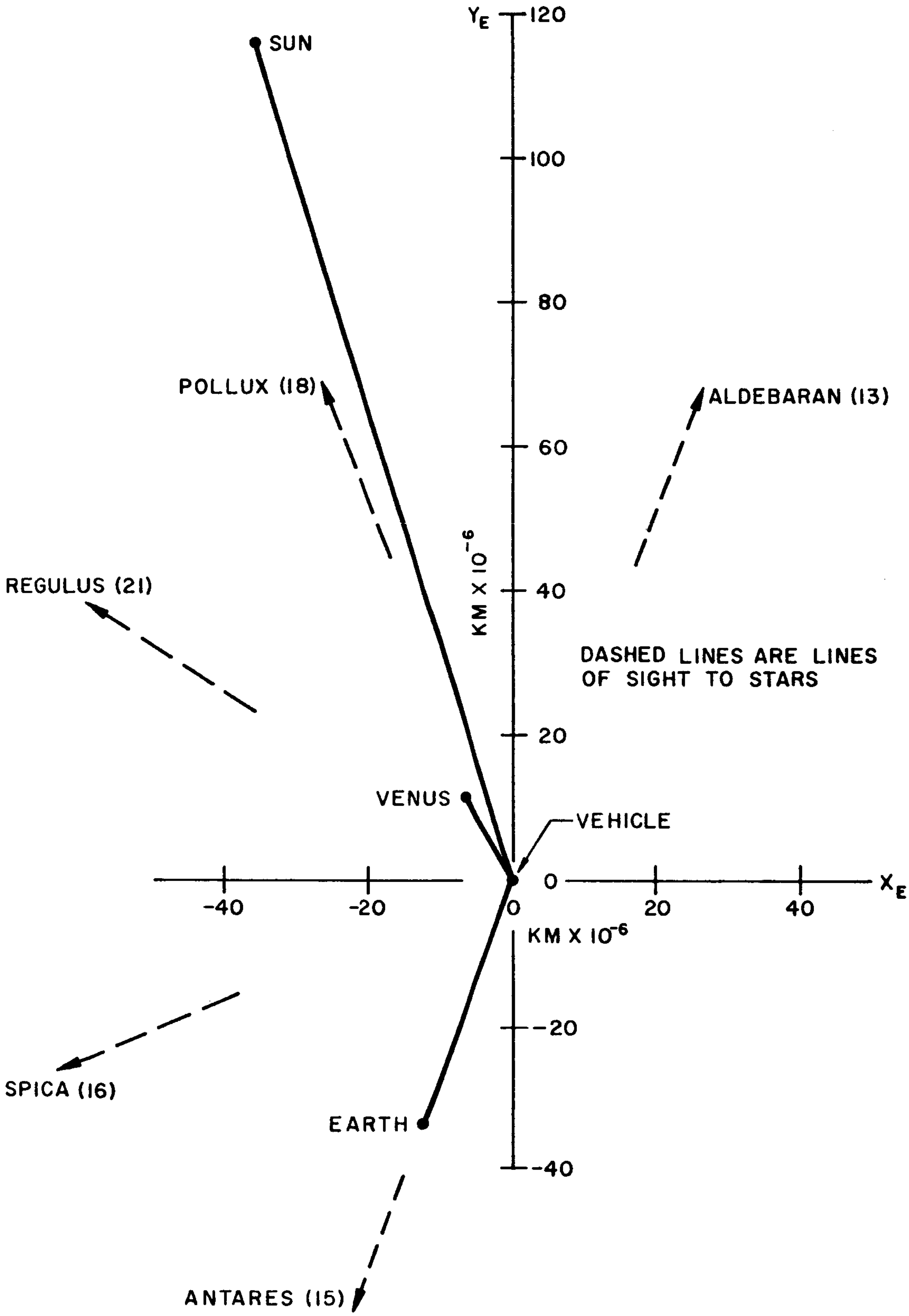

Fig. 3. Projection in ecliptic plane of near bodies and lines of sight to "in-plane" stars.

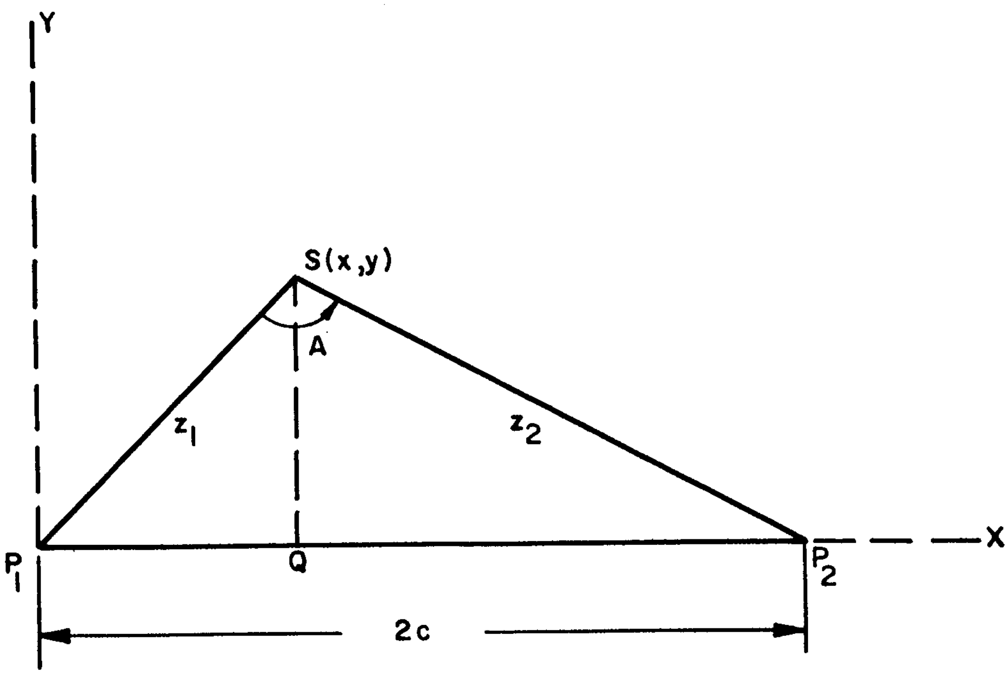

S:	space ship position
P_1, P_2:	near body positions
$A = \measuredangle P_1 S P_2$:	angle to be measured

Fig. 4. Measurement of the angle between two near bodies.

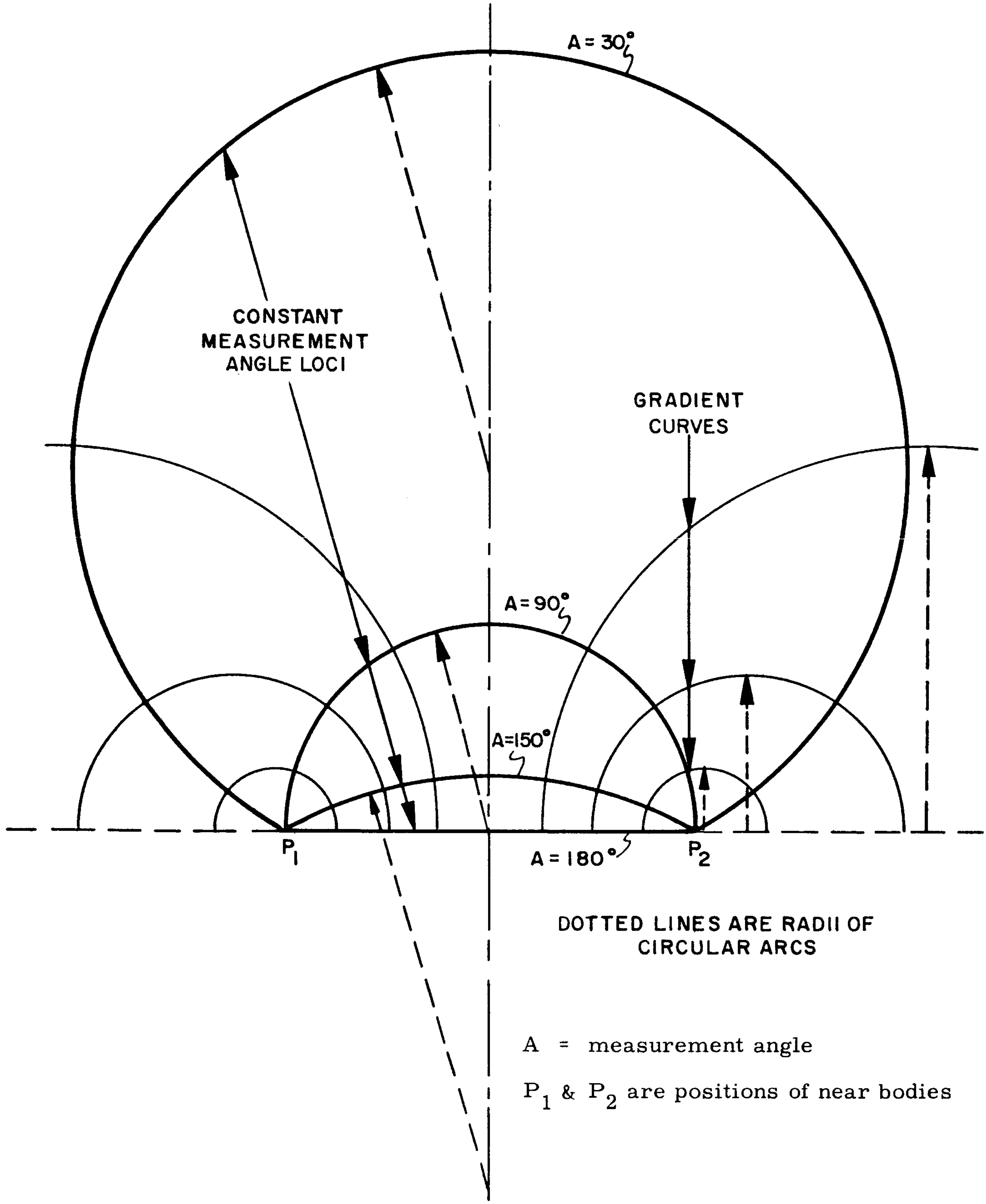

A = measurement angle

P_1 & P_2 are positions of near bodies

Fig. 5. Constant-measurement-angle loci and gradient curves for the angle measured between two near bodies.

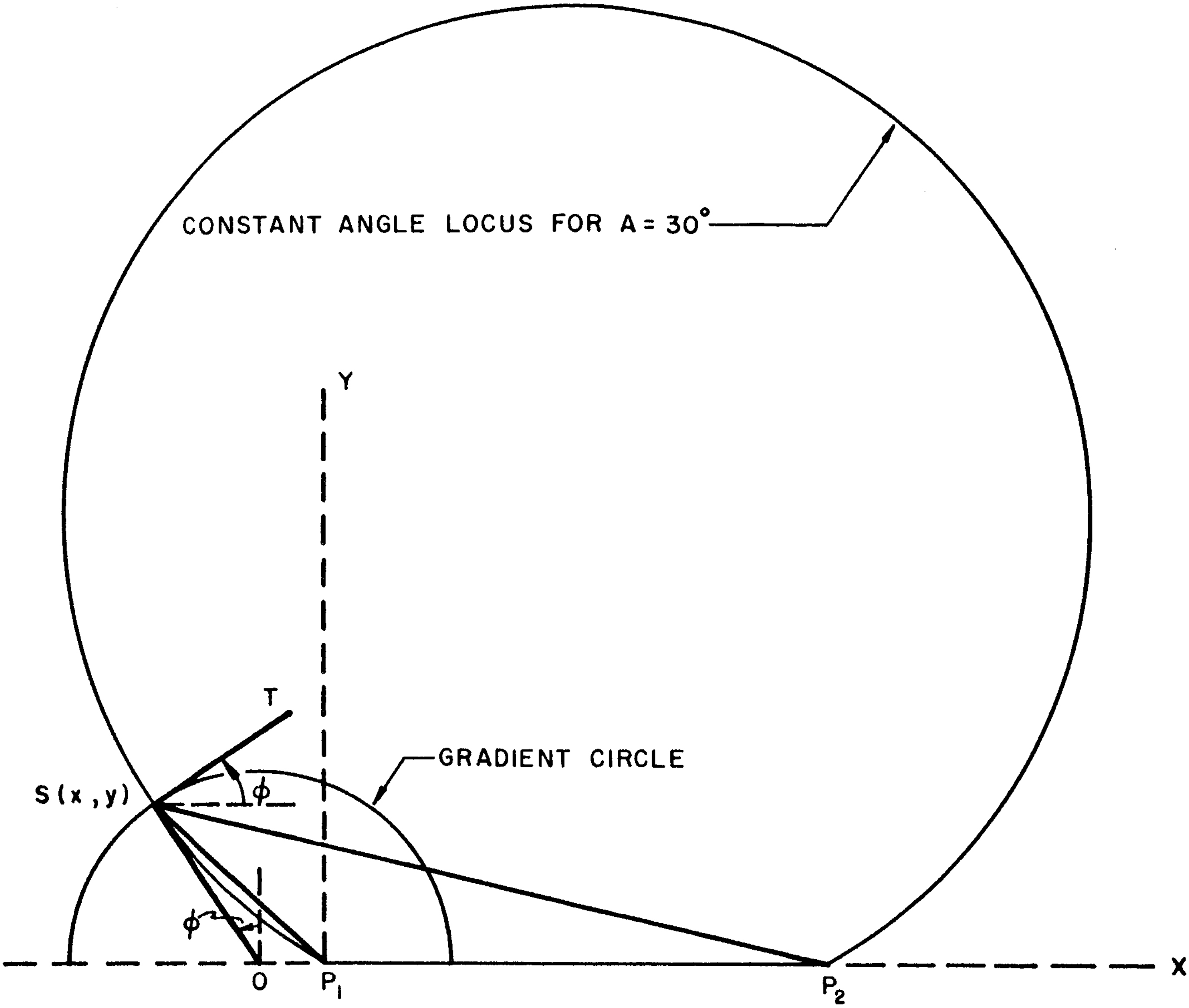

OS = R = radius of gradient circle

= tangent to locus at S

ST = tangent to gradient circle at S

ϕ = angle between X-axis and ST

= angle between Y-axis and OS

Fig. 6. The angle ϕ.

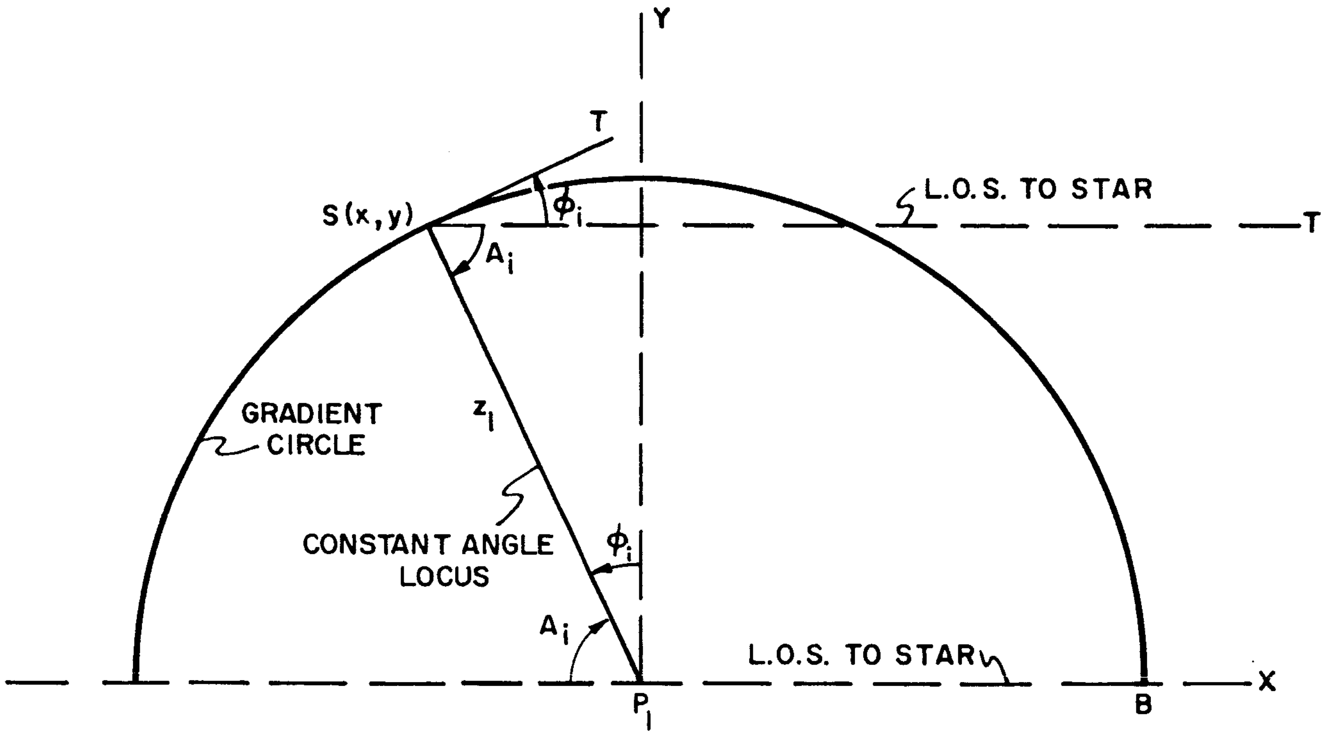

L. O. S. = line of sight

S = space ship position

P_1 = near body position

A = measurement angle

z_1 = SP_1 = distance from space ship to near body

$$A_i + \phi_i = \frac{\pi}{2}$$

Fig. 7. The angle measured between a near body and a star.

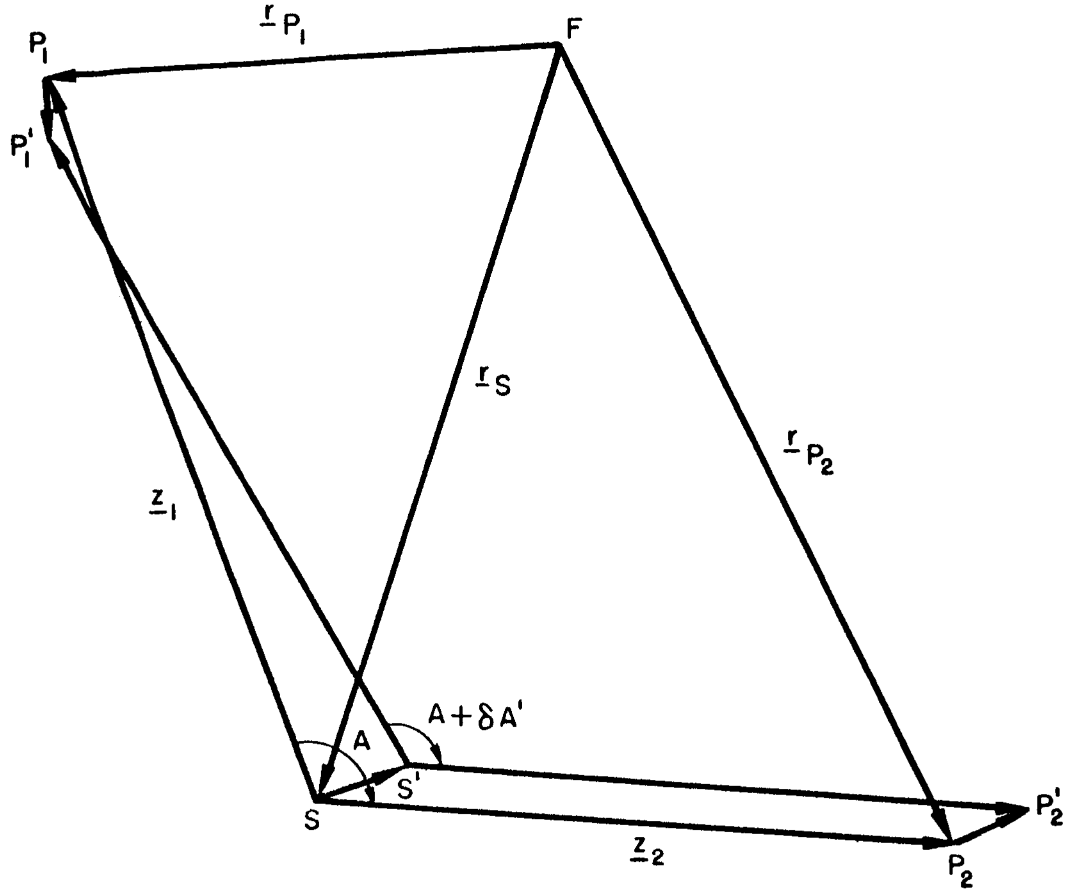

F	-	position of the sun
S	-	position of space vehicle on reference trajectory at time t
S'	-	position of space vehicle on actual trajectory at time $(t + \tau)$
P_1	-	position of first near body at time t
P_1'	-	position of first near body at time $(t + \tau)$
P_2	-	position of second near body at time t
P_2'	-	position of second near body at time $(t + \tau)$
A	-	nominal value of angle to be measured at time t
$A + \delta A'$	-	angle actually measured at time $(t + \tau)$

Fig. 8. Comparison of actual and nominal measurements for angular sighting between two near bodies.